Recent advances in the BRAMS network

Hervé Lamy[1], Michel Anciaux[1], Sylvain Ranvier[1], Stijn Calders[1], Emmanuel Gamby[1], Antonio Martinez Picar[2] and Cis Verbeeck[2]

[1] **Belgian Institute for Space Aeronomy, Avenue Circulaire 3, 1180 Brussels, Belgium**
Herve.lamy@aeronomie.be, Michel.anciaux@aeronomie.be,
stijn.calders@aeronomie.be, emmanual.gamby@aeronomie.be,
sylvain.ranvier@aeronomie.be

[2] **Royal Observatory of Belgium, Avenue Circulaire 3, 1180 Brussels, Belgium**
Antonio.martinez@oma.be, cis.verbeeck@oma.be

BRAMS is a radio network using forward scattering techniques to detect and characterize meteoroids falling into the Earth's atmosphere, roughly above Belgium. In this article the most recent advances in the BRAMS network and analyzing BRAMS data are presented. First, a calibrator that has been added to all receiving stations is described. It aims at providing a reference for both amplitude and frequency. The importance of this calibrator in future analysis of underdense meteor echoes is explained. Second, a description of the interferometer in Humain is provided as well as details of future calibration using a UAV and the calibrator. Finally, tests of the method proposed by Roelandts (2014) for automatic detection of meteor echoes in BRAMS data are discussed.

1 The BRAMS network

BRAMS (Belgian RAdio Meteor Stations) is a radio network using forward scattering techniques to detect and characterize meteoroids falling into the Earth's atmosphere, above Belgium and neighboring countries. It consists of a dedicated transmitter located in Dourbes (South-East of Belgium) and in ~ 25 receiving stations located in Belgium. The transmitter (Tx) is a crossed dipole antenna with a reflecting metallic grid of 8m × 8m, emitting a pure sine wave at a frequency of 49.97 MHz with a total power of 150 watts.

All BRAMS receiving stations (Rx) are using a three-element Yagi antenna and an ICOM-R75 receiver for the reception chain. The received signal is shifted in frequency from 49.97 MHz to ~1 kHz using the local oscillator (LO) of the receiver. A Garmin GPS 18x LVC Sensor provides a PPS (Pulse Per Second) which ensures time synchronization between the various BRAMS receiving stations. The shifted signal coming from the receiver and the signal from the GPS receiver are sampled simultaneously by a USB external sound-card BERINGHER UCA222 and stored on a local PC. The frequency stability of the LO is not very good such that the frequency carrier can drift a lot (typically ~ 100-200 Hz) depending on the local temperature.

2 New calibrator for the BRAMS stations

In 2015, a new calibrator has been added to each station with the goals of monitoring the gain and frequency drifts. This calibrator, designed at BISA, emits a signal of known frequency and amplitude and is fed into the receiver via a Tee connector. It is powered by micro-USB. *Figure 1* is a schematic of the new receiving chain of a BRAMS station *while Figure 2* shows the calibrator and how it is inserted in the reception chain.

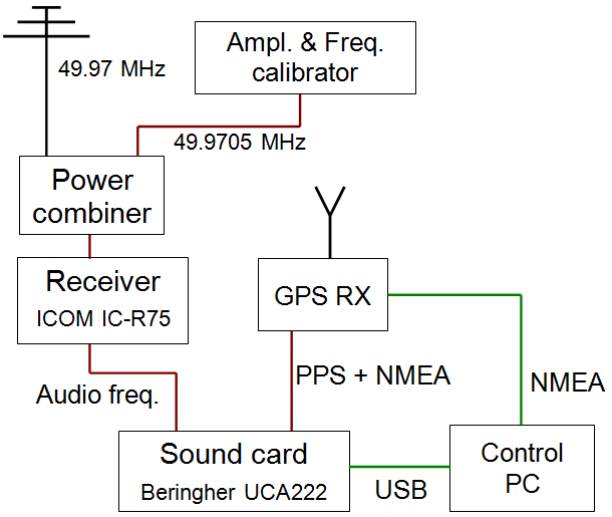

Figure 1 – Schematic of the reception chain of a BRAMS station including the new BRAMS calibrator.

The power level of the inserted signal is of -130 dBm (=10^{-16} W) and can be controlled by software with steps of 3dB. It provides a S/N ratio > 20 dB in a 0.3 Hz band which is the typical frequency resolution used in BRAMS spectrograms. The frequency of the signal is 49.97050 MHz such that the signal appears 500 Hz above the beacon frequency in the audio band. This frequency can be modified in order to appear in a region of the receiver band where no (trail) meteor echo occurs. The internal frequency reference using a Temperature Controlled Crystal Oscillator ensures a much better frequency stability (a few Hz) than the LO in the receiver. Since the signals of the BRAMS calibrator and from the antenna are combined in front of the receiver, the frequency drift of the LO affects both signals in the same way.

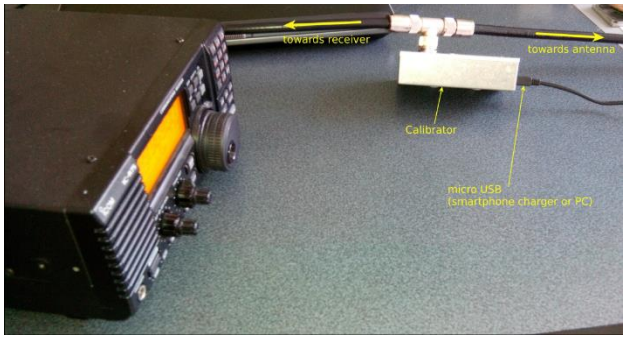

Figure 2 – New BRAMS calibrator inserted in the reception chain.

Figure 3 shows an example of a spectrogram obtained with the new reception chain. The carrier frequency appears around 1190 Hz with several airplane and meteor trail echoes within ± 50 Hz. The fact that the carrier does not appear at 1 kHz is due to the inaccuracy of the LO of the receiver. The horizontal line at around 1690 Hz is the signal coming from the calibrator and is shifted in frequency by the same amount as the carrier. Therefore the first utility of the calibrator is to provide a frequency reference which allows to easily identify frequency drifts of the beacon. It is particularly important when the beacon is barely or not visible at all in some receiving stations due either to some obstructions in the main lobe of the antenna or to bad tropospheric conditions for wave propagation.

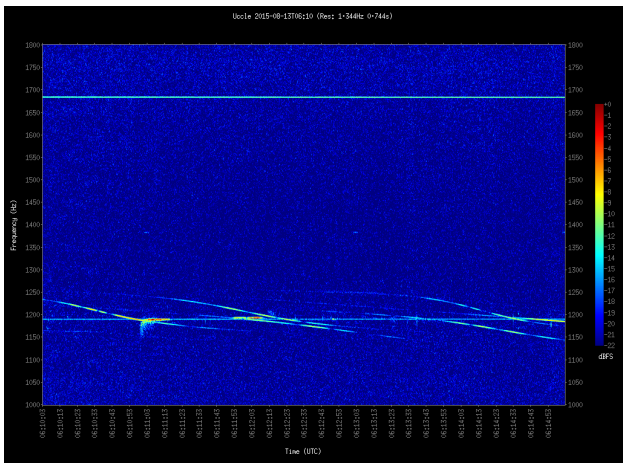

Figure 3 – Spectrogram obtained at BEUCCL station on 13 August 2015 at 06:10 UT. Time duration (horizontal axis) is 5 minutes and the frequency range (vertical axis) is [1000-1800] Hz. The signal from the calibrator (horizontal line 500 Hz above the frequency of the carrier) is clearly visible.

Another future important application of the calibrator will be to provide an amplitude reference. This will be useful for the study of the profiles of underdense meteor echoes, which consist of a sudden rise of the received power until it reaches a peak, followed by an exponential decay. The formula for the peak can be found e.g. in the classical textbook of McKinley (1961), page 239. It depends on geometrical factors (e.g. the scattering angle or the inclination of the meteor trajectory with regard to the wave propagation plane), on "controlled" factors (power transmitted, wavelength, gains of the transmitting and receiving antennas), on the polarization angle of the reflected radio wave and on the ionization (electron density) at the reflection point. To retrieve meteoroid trajectories from multi-station observations is one of the primary goals of the BRAMS network and is currently under way with the METRO project[1]. This will provide the geometrical factors. The directional patterns of the gains of some of the BRAMS antennas are currently measured using a UAV (Unmanned Aerial Vehicle) with the BRAMS calibrator as payload acting as a transmitter (Martinez Picar et al., 2014; 2015). For the remaining antennas for which this calibration will not be possible (e.g. because we do not have authorization to fly the UAV), a theoretical pattern will be used instead. The polarization angle of the meteor echoes can only be measured using crossed Yagi antennas (which will be the case in at least 2 stations). Otherwise a "reasonable" value should be taken, e.g. based on the statistical distributions of the polarization angles of meteor echoes received at the 2 stations above. Once all these parameters are measured, the peak value of underdense meteor echoes is directly related to the electron density at the specular reflection point of the meteor trail. Since the position of this point varies for different geometries Tx-Rx, several values of the electron density along the meteor trail can be obtained using multi-station observations of a given radio meteor. These values can be compared to predictions of an ablation model (using speed and incidence angle values coming from our observations) to provide an estimate of the mass of the meteoroid.

3 Interferometric station in Humain

The receiving station located in Humain (South-East of Belgium) is an interferometer using five three-element Yagi antennas located along two orthogonal axes following the design of Jones et al. (1998). The central antenna is a crossed Yagi antenna (able to measure the polarization angle of the incoming meteor echoes) so in total there are 6 antennas. By measuring the phase differences between three antennas along each axis, the direction of arrival of the meteor echo can be measured unambiguously and with an accuracy of ~ 1°. The block diagram of the interferometer is given in *Figure 4*.

Contrary to other receiving stations, the interferometer uses more expensive receivers (AR-5001D) which include a 10 MHz reference input to ensure frequency coherence and stability. A 10 MHz distribution is sending the reference signal to all 6 receivers. Unfortunately these receivers are not phase coherent, meaning that after power has been switched off (e.g. due to power failure), they start again with a random phase. The frequency/amplitude calibrator described in section 2 is therefore used to inject a signal to the 6 receivers in order to guarantee a continuous knowledge of their phase relation. A more sophisticated ADC is replacing the USB sound-card and samples the seven signals simultaneously (6 receivers and the GPS receiver).

[1] http://brams.aeronomie.be/metro

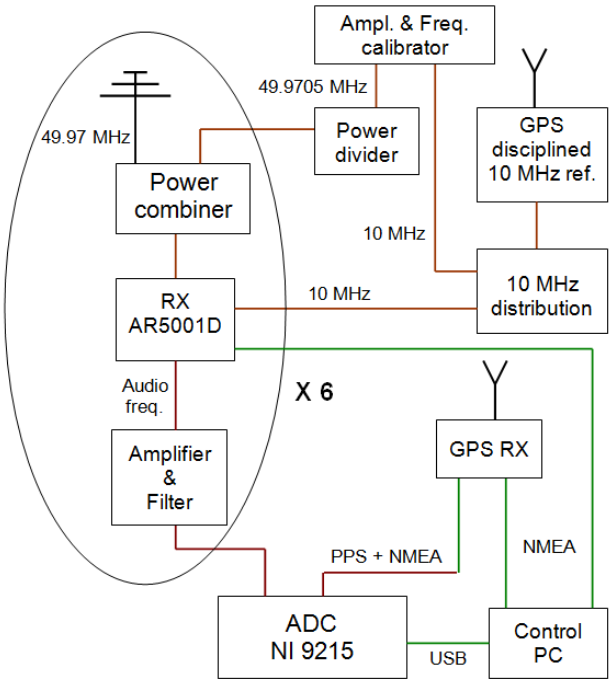

Figure 4 – Schematic of the interferometer in Humain.

Data from the interferometer are now routinely acquired. The next step will be to check the whole system by using a transmitter located at a known location and the algorithm described in Jones et al (1998). For that purpose, the BRAMS calibrator and a simple monopole antenna will be added as payload to the UAV used for measuring the directional pattern of the BRAMS antennas. The drone will fly around the interferometer and the GPS receiver onboard will provide its approximate position at a given time. By selecting a frequency with no other sources nearby, the signal from the calibrator can be easily identified in the data from the receivers and phase differences will be calculated to obtain the direction of arrival of the signal. Several positions will be considered to calibrate the algorithm.

4 Tests of the automatic detection algorithm of Roelandts

With each of the 25 receiving stations producing 288 files of 5 minutes duration per day, the BRAMS network generates more than 7000 files daily. A receiving station detects typically 1500-2000 meteor echoes depending on the sensitivity of the reception chain. Such a huge amount of data requires the use of automatic detection algorithms for meteor echoes. The difficulty comes mostly from the presence of reflections on many airplanes that superimpose on meteor echoes. In the past few years, several attempts to develop reliable and efficient automatic detection algorithms were proposed using either the spectrogram or the raw audio signal (see Calders & Lamy, 2014, for a review).

One promising method was proposed by Tom Roelandts during IMC 2014 (Roelandts, 2014). From a filtered version of the raw audio signal, this method computes an indicator signal, which is roughly the ratio of the energy contents in a short duration window (a fraction of a second) and in a large duration window (a few seconds). The idea is that underdense meteor peaks contribute strongly to the energy content in the short window but not to the long one, while airplane echoes will do the opposite. Hence the indicator signal should display peaks at the location of the underdense meteor echoes while the plane echoes should be mostly smoothed out. A threshold is then applied to detect these peaks.

To test this method in more detail, several sets of data have been carefully analyzed by several experienced users and meteor echoes have been manually counted on the corresponding spectrograms in order to create a reference database. To illustrate results of the tests, data from the Ottignies station obtained on 15th March 2015 between 00:00 and 01:00 UT are used here. This set of data contains barely any airplane echoes and can therefore be considered as "simple", the difficulty being linked mostly in detecting faint meteor echoes with a S/N ratio close to 1. 120 meteor echoes have been counted manually for the total of the 12 spectrograms.

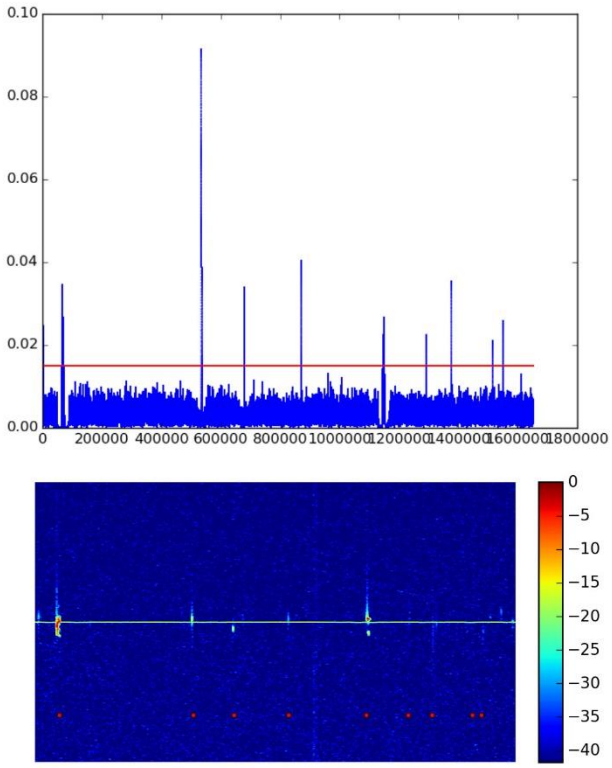

Figure 5 – Example of results obtained using the method of Roelandts (2014) for the data from Ottignies obtained at 00:15 UT on 15 March 2015. Top panel : signal indicator as function of time (in number of samples). Bottom panel : spectrogram with detections added as red dots.

The method of Roelandts uses 3 important parameters: P1, the length of the short window, P2 the length of the large window, and P3 the value of the threshold. In *Figure 5*, an example is shown for data obtained at 00:15 UT. Top panel shows the indicator signal while bottom panel shows the spectrogram and the peaks detected in the indicator signal (red dots). These results have been obtained with "default" parameters proposed by

Roelandts (2014) for P1 ~ 0.02 sec and P2 ~ 5.45 sec. A threshold value P3 ~ 0.015 is used.

In *Figure 6*, the results obtained varying the threshold value P3 are presented. The absolute values of the threshold are unimportant here and so arbitrary units are used. The number of detected meteor echoes (blue curve), false negatives (real meteor echoes missed by the method, green curve) and false positives (other signals that are mistakenly counted as meteor echoes by the method, red curve) are divided by the total number of meteor echoes in the reference database and therefore provided as percentages. The blue and green curves are complementary and their sum gives 1.

As expected, when the threshold increases, the percentage of detection decreases since only the largest peaks corresponding to the brightest meteor echoes are then detected. The maximum of the blue curve is around 90%. The decrease observed in the left hand part of the maximum is due to an additional trick used to count peaks in the method. Indeed, the indicator signal may display a complex behavior with many fast oscillations and within one "apparent" peak, it can quickly go up and down the threshold value several times. In order to avoid incorrectly considering this as several meteor echoes, a criterion is applied to group these peaks and count them only as one if two consecutive peaks are not separated by at least 1 second. This seemingly arbitrary value is chosen empirically as meteor echoes very rarely appear so close to each other. When the threshold is too low (below ~ 8 in *Figure 6*), it detects many of these false peaks and as a consequence several real meteor echoes are "merged", decreasing the number of detections. This makes the left hand part of the results in *Figure 6* meaningless.

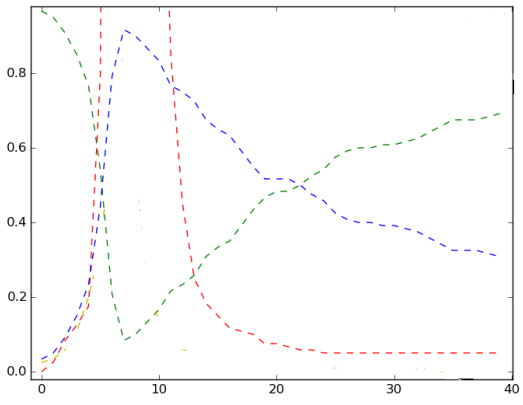

Figure 6 – Test of the method proposed by Roelandts using data from Ottignies station obtained on 15 March 2015. The horizontal axis is the value of the threshold (in arbitrary units) while the vertical axis is the number of detections divided by the total number of meteor echoes in the reference database. The blue curve is the percentage detection of meteor echoes, the green curve is the percentage of false negatives and the red curve represents the percentage of false positives.

The problem of choosing the most appropriate value of the threshold parameter is complicated by the large number of false positives that appear when the threshold becomes too low. Too many small peaks are generated and comparable to those due to the weakest meteor echoes. Therefore decreasing the threshold help detecting the latter ones but this is done at the expense of increasing the number of false detections. In *Figure 6*, the red curve increases very quickly when the threshold becomes smaller than ~ 15 so smaller values should not be considered. The problem is that for a threshold value of 15, the percentage of detection is only of ~ 65%. Note that the plateau reached by the red curve for large values of the threshold is due to broad-band interference which can be easily removed from the data before processing them with this method.

More analysis will be provided elsewhere, including varying the other two parameters P1 and P2 to find the optimal set of parameters in a three-dimensional parameter space, tests with more data and tests using an adaptive threshold (following approximately the large scale variations of the indicator signal). The current conclusion is that even with simple data, the method is not so easy to use. The choice of the adequate threshold parameter is complicated by the large number of false negatives that can be generated.

5 Conclusions and perspectives

In this paper two important hardware additions to the BRAMS network have been described, namely the new frequency/amplitude calibrator added to each receiving station and the interferometer located in Humain. The first one will allow accurate determination of frequency drifts and of amplitude peaks of underdense meteor echoes. The latter will provide a precise determination of the direction of arrival of meteor echoes, which will be useful for the retrieval of meteoroid trajectories.

Regarding the data, the method proposed by Roelandts (2014) has been tested on several sets of data for which an accurate manual count is available. One case study is presented in this paper, the rest will be published elsewhere. A preliminary conclusion is that the method might not be able to provide a sufficiently high detection rate without being contaminated by too many false detections. More analysis is of course mandatory before confirming this conclusion. In parallel new methods are continuously investigated.

Acknowledgment

The main author would like to thank Arno Van Thiegem (student from ULg) for his nice and enthusiastic work while doing his summer job at BISA. Many thanks as well to Tom Roelandts for taking time and providing excellent discussions about the use of his method.

References

Calders S. and Lamy H. (2014). "Automatic detection of meteors in the BRAMS data". In Rault J.-L. and Roggemans P., editors, *Proceedings of the*

International Meteor Conference, Giron, France, 18-21 September 2014. IMO, pages 194–196.

Jones J., Webster A. R. and Hocking W. K. (1998). "An improved interferometer design for use with meteor radars". *Radio Science*, **33**, 55–65.

Martinez Picar A., Ranvier S., Anciaux M. and Lamy H. (2014). "Modelling and calibration of BRAMS antenna systems". In Rault J.-L. and Roggemans P., editors, *Proceedings of the International Meteor Conference*, Giron, France, 18-21 September 2014. IMO, pages 201–206.

Martinez Picar A., Ranvier S., Anciaux M. and Lamy H. (2015). "Directional pattern measurement of the BRAMS beacon antenna system ". In Rault J.-L. and Roggemans P., editors, *Proceedings of the International Meteor Conference*, Mistelbach, Austria, 27-30 August 2015. IMO, pages 177–179.

McKinley D. W. R. (1961). "Meteor Science and Engineering". McGraw-Hill Book Company New-York U.S.A.

Roelandts T. (2014). "Meteor detection for BRAMS using only the time signal". In Rault J.-L. and Roggemans P., editors, *Proceedings of the International Meteor Conference",* Giron, France, 18-21 September 2014. IMO, pages 197–200.

The author, *Hervé Lamy*, during his lecture (Photo by *Axel Haas*).